Carrier Diffusivity in Porous Membranes

Yuria Saito,*,† Kenichi Hirai,† Hideyuki Emori,‡ Shuuhei Murata,‡ Yoshihiro Uetani,‡ and Keisuke Kii‡

National Institute of Advanced Industrial Science and Technology, 1-8-31, Midoragaoka, Ikeda, Osaka 563-8577 Japan and Nitto Denko Corporation, 1-1-2, Shimohozumi, Ibaraki, Osaka 567-8680 Japan

Received: August 25, 2003; In Final Form: November 4, 2003

Carrier diffusivity of a lithium electrolyte solution in porous membranes was evaluated by observation of diffusion behavior of ionic species using NMR spectroscopy. We performed analysis on the basis of the restricted diffusion model and a new idea of diffusion distribution. That new concept is engendered in the assumption that observed diffusion values are distributed according to pore size distribution and nonuniformity of pore and polymer density in a membrane. Carrier diffusivity in polyethylene (PE) porous membranes showed characteristic echo attenuation, which differs from echo behavior as a result of random walk migration. We first tried to simulate the echo change on the basis of the restricted diffusion model in porous structure, resulting in disagreement with the observed echo change. As a result, the idea that diffusion values are distributed concurrent with porous geometry was applied to interpret the situation. Introduction of a Gaussian function to represent the distributed condition yielded highly reproducible results for the membranes. Carrier diffusivity in porous PVDF membranes showed a narrow distribution compared with that of PE membrane. The swelling feature of the PVDF polymer would contribute to averaging the pore size and preparing the uniform network for carrier transport pathway.

Introduction

Carrier mobility is an essential property for conductive materials such as electrolytes and electrodes in electrochemical devices. Diffusion behavior of the species reflects not only features of the carrier itself, but also features of the medium through which the carrier migrates as well as the interactive effects between the carrier and medium. This means that carrier diffusivity can be used as an indication to evaluate the structural feature of the medium. In practice, investigation of diffusion or transport mechanism is necessary for the field of filtering and separating technology.

The separator membrane, a component of battery devices, is a typical material that the carrier mobility in it dominates the battery performance.[1] The membranes have a porous structure, typically comprising 10−30-μm-thick polyolefin film with 0.1−1-μm pore size, depending upon the individual purpose for usage. This morphological feature is associated with the carrier mobility. The separator membrane serves to separate the anode and cathode to prevent short-circuiting. Pore spaces, which are connected with each other and filled with an electrolyte solution, provide conduction paths for ionic species. For high battery performance, ionic mobility must be kept as high as possible even in the convoluted paths of the porous structure.

To obtain high diffusivity in the porous membrane, physical geometry of the medium must be optimized as follows: (1) high porosity (large amount of space) to hold a large content of electrolyte solution; (2) profitable connection of the pores for efficient transport of carriers; and (3) uniformity of the pores, implying the narrow distribution of pore size, to provide a constant diffusion coefficient of carriers throughout the membrane. Porosity and pore linkage must also be considered from the aspect of safety in battery devices as restricting the charge-transfer reaction if necessary, which sometimes conflicts with the course of conductivity enhancement.[2] The third point, geometrical uniformity, correlates with cyclic performance of the charge and discharge reactions in the battery. If diffusivity differs depending on the point or region in a membrane, a mass concentration gradient would be promoted in the progress of charge and discharge cycles because of the difference in carrier migration rate on the position. This situation is more serious for high-rate performance. However, from a practical aspect, it is impossible to equilibrate pore sizes exactly because the pores are introduced in the membranes at the expanding process of the polymer matrix, resulting in the pore size distribution.

Thus far, two independent approaches have been used to evaluate the performance of porous membranes. Carrier migration property in the membrane was observed through measurements of electrochemical conductivity of ionic species and the aeration and transmission degrees of gas and liquid. On the other hand, porous geometry was evaluated by measuring porosity and pore size distribution on the basis of gas adsorption and gas transmission techniques. We anticipate that carrier diffusivity can be directly interpreted as a function of the geometrical feature of the medium. To achieve this, it is indispensable to measure the carrier diffusivity and analyze it on the basis of some geometrical factor.

We have used the NMR technique for diffusion coefficient measurement of ion conductive materials to investigate the carrier migration mechanism.[3−5] One advantage of this approach is that structural features of media can be reflected in the observed echo signal by selecting an appropriate measurement condition. A typical diffusive feature illustrating this situation is called restricted diffusion behavior, which has been discussed

* Corresponding author. Tel: +81-72-751-9618; fax: +81−72−751−9714; e-mail: yuira-saitou@aist.go.jp.
† National Institute of Advanced Industrial Science and Technology.
‡ Nitto Denko Corporation.

10.1021/jp0365256 CCC: $27.50
Published on Web 12/20/2003

systematically.[6−8] In this case, NMR echo decay, which can be detected by application of gradient pulses for diffusion measurement, shows characteristic oscillation that is entirely different from the echo-changing behavior attributed to random walk migration. We previously reported restricted diffusion in polymer electrolytes, which was a first observation and analysis of anomalous diffusive feature in practical materials.[9] Ionic species interact with the sites on the polymer in polymer electrolytes. They hop from site to site on the polymer taking advantage of segmental motion of the polymer chains.[10,11] An appropriate-range migration behavior in the polymer depends on the degrees of entanglement of the chains and the size of a domain structure. The domain is a micron-size mass of the entangled polymer chains and a unit structure of restricting the free migration of carriers extricating from the mass. Consequently, anomalous echo change of restricted diffusion which reflects the size and geometry of the diffusing space can be observed.

Analogously with the polymer electrolytes, carrier migration in the porous structure can be restricted because of the convoluted transport pathways that comprise interconnected pores.[12] The restricted condition in migration is affected by pore size, porosity, pore linking condition, and chemical effect of the porous medium on the carriers.

Anomalous behavior of the echo signal in diffusion measurement, if it appears, is a clue to evaluate structural features of the medium for carrier transport. In this study, we attended to carrier diffusivity in separator membranes. Here, we propose a new approach for interpreting the carrier diffusivity in the porous structure on the basis of the concept of diffusion distribution. We applied the idea to two types of separator membranes to confirm the validity of the model for practical materials: one is polyethylene (PE); the other is polyvinylidene fluoride (PVDF). These materials contrast with each other in terms of their swelling condition with nonaqueous electrolyte solutions. This approach suggests a straightforward direction to investigate the carrier migration mechanism and thereby develop the intended materials according to the essential mechanism.

Experimental Section

Polyvinylidene fluoride (PVDF) type membranes (Durapore) of averaged pore size, 0.1 μm and 5 μm, and film thickness of around 50 μm were purchased from Millipore Co. Polyethylene (PE) type porous membranes were prepared using starting materials of polyethylene ($M = 1.5 \times 10^6$) as main chains, unsaturated rubber for reinforcement, and thermoplastic elastomer which plays a role of shutting the ion transfer by melting in case of unusually heated condition. The mixture of a definite fraction was mixed with paraffin to form a slurry condition at 160 °C. It was then put on a metal board to quench to 0 °C. The quenched polymer matrix was heat-pressed at 115 °C to 0.9-mm thickness following stretching in both directions and then desorbing the solvent. Stretching was also performed after desorbing paraffin to prepare a porous membrane with larger pore size. The thickness of both films, stretched with and without paraffin, was around 15 μm. Dried porous membranes of PVDF and PE were immersed into the electrolyte solution of 1.4 M $LiPF_6$ dissolved in the mixed solvent of ethylene carbonate (EC) and ethyl methyl carbonate (EMC) (1:1 in volume ratio) for a week to fill the pores completely with the solution. Full occupation of the solution into the membranes to be equilibrium condition was confirmed from the impedance measurement of the membranes with immersing time into the solution. PE membranes reached equilibrium state in a minute and PVDF membranes took 5 days to be stabilized condition as swollen polymer after immersing. The thickness of the PE membranes with solution was slightly greater than 15 μm but not changed so much because of no swelling feature of PE polymer substrate. For diffusion measurement of separator samples, the solution on the surface was carefully wiped away to remove the effect of residual solution at the membrane surface. About 20 sheets of membranes were overlapped to set in the NMR tube perpendicular to the direction of the magnetic field for diffusion measurement, indicating that observation of diffusion was made across the plane.

Diffusion coefficients of the cation, anion, and solvent species in the membrane were measured by the pulsed gradient spin−echo NMR (PGSE-NMR) technique with probed nuclei of ^{7}Li (116.8 MHz) for the cation, ^{19}F (282.7 MHz) for the anion, and ^{1}H (300.5 MHz) for the solvent species using a JBM-ECP300W wide bore spectrometer.[3] This study used the stimulated echo sequence for this application. The half-sine-shaped gradient pulse was applied twice in sequence after the first and third 90° pulses to detect attenuation of echo intensity of the probed species.[13,14] Typical values of field gradient pulse parameters were $g = 2.5-10$ T/m for pulse strength, $\delta = 0-5$ ms for the pulse width, and $\Delta = 80$ ms for the interval between the two gradient pulses. Δ was shifted to 30 ms and 160 ms in case of examining the diffusion time dependence on the echo-changing behavior.

Formulation of Carrier Diffusivity in Some Media. Carrier diffusion behavior reflects chemical and physical features of the medium in which the carriers move. In this section, we classify observed NMR echo signal behavior during the diffusion measurement according to the morphology of the medium.

Ionic species of the salt and solvent species in a solution follow Brownian motion colliding randomly with each other. This behavior displays a spin−echo intensity change observed in PGSE-NMR techniques expressed as

$$M/M_0 = \exp[-\gamma^2 g^2 \delta^2 D(4\Delta - \delta)/\pi^2] \qquad (1)$$

where D is the diffusion coefficient of the species, γ is the gyromagnetic ratio, g is the gradient pulse strength, δ is the pulse width, and Δ is the interval between the two gradient pulses in the sequence.[3] Assuming that Δ and g are constant and $4\Delta \gg \delta$, this relation indicates that the log-plot of intensity, as a function of δ^2, provides a linear change having a slope proportional to the value of the diffusion coefficient. If several phases exist in a sample and each phase has independent diffusivity represented by eq 1, the observed echo change can be extended as

$$M/M_0 = \sum_i a_i \exp[-\gamma^2 g^2 \delta^2 D_i(4\Delta - \delta)\pi^{-2}] \qquad (2)$$

where a_i is a normalized prefactor implying the existing population of i-phase. Ideally, diffusion coefficients of i components can be deduced from different slopes in a log-plot of intensity.

In case that the probed species are subject to some restriction in migration caused by chemical or geometrical effects from the surroundings, migration feature deviates from the random walk behavior represented by eqs 1 and 2. This situation is recognized as "restricted diffusion". Its typical behavior has been studied theoretically for some ideal model structures.[7,12] For example, in a rectangular box, carriers are bounded by the barrier of walls of the box during migration and the echo signal in

one-dimensional diffusion is described as

$$M(q,\Delta) = \frac{2[1-\cos(2\pi qa)]}{(2\pi qa)^2} + 4(2\pi qa)^2 \sum_{n=1}^{\infty} \exp\left(-\frac{n^2\pi^2 D\Delta}{a^2}\right) \times \frac{1-(-1)^n\cos(2\pi qa)}{[(2\pi qa)^2-(n\pi)^2]} \quad (3)$$

where $q = (2/\pi)(\gamma\delta g/2\pi)$ for the sine-shaped gradient pulse and a is the width of the rectangular box.[12] In the range of appropriate parameters, this formula yields an oscillating change in log M versus δ^2 in which the oscillation cycle is dominated by a.[9] Furthermore, an extended model in which the carrier migration in porous structure comprising interconnected pores was proposed by Callaghan.[12] The signal intensity for the carrier migration in an array of interconnected pores is proposed as

$$M(q,\Delta) = |S_0(q)|^2 F(q,\Delta)$$

$$S_0(q) = \int_j \rho_0(z'-z_j)\exp[i2\pi q(z'-z_j)]dz'$$

$$F(q,\Delta) = \exp\left(-\frac{4D_{\text{eff}}\Delta}{b^2}\sin^2(\pi qb)\right) \quad (4)$$

where b is the mean spacing between pores and D_{eff} is the description of the diffusion coefficient of the long-range permeation of the pore matrix by species undergoing Brownian motion.[12] This model also showed a characteristic oscillating or monotonically curved feature in which the oscillation cycle depends on a (pore size) and b.[9]

We have already observed and investigated the restricted migration behavior of ionic species in PEO-type polymer electrolytes showing a typical oscillating behavior in spin−echo attenuation.[9] It is presumed that the causes of restriction are (1) microscopic ion transport mechanism of hopping on the fixed sites of polymer chains and (2) macroscopic domain structures of entangled polymer chains from which the carrier cannot be extricated easily.

We suppose that the deviation from random walk behavior in a porous medium reflects not only the local space geometry proposed above, whose contribution to the echo attenuation could be controlled by measuring time, Δ, but the overall geometry of the porous structure. As suggested by Callaghan, carrier migration behavior in the porous structure can be recognized as Brownian motion when we consider a long-range migration of carriers passing through several interconnected pores in all directions.[12] That motion can be described by an effective diffusion coefficient, D_{eff}, even if the carriers are locally restricted in diffusion. This view is based on the assumption that D_{eff} is the same in any location of a porous structure. However, in practice, pore size and polymer chain density vary according to location in a membrane, implying geometrical nonuniformity of the membrane. This would result in distribution of D_{eff} in the observed region in a sample. We would like to deal with this situation by introducing a distribution function. We express the spin−echo change on the analogy of eq 2 as

$$M/M_0 = \sum_i a_i \int f(D)\exp[-\gamma^2 g^2\delta^2 D_i(4\Delta-\delta)\pi^{-2}]dD$$

$$f(D) = \sqrt{\frac{1}{2\pi\sigma^2}}\exp\left[-\frac{(D-D_0)^2}{2\sigma^2}\right] \quad (5)$$

where $f(D)$ is the distribution function, D_0 is the averaged value of diffusion coefficients, and σ is the standard deviation of diffusion coefficients. This evaluation shows mobility of the carrier species from D_0 and morphological uniformity of the host medium from σ, simultaneously. The next section elucidates the characteristic echo attenuation behavior of the carrier diffusion process in practical membranes by the application of the models.

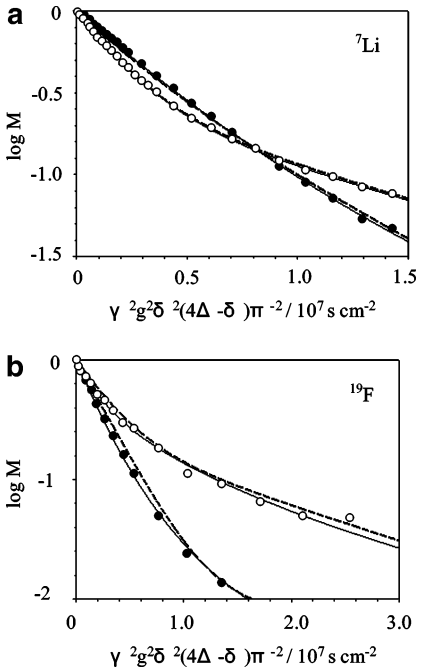

Figure 1. NMR spin−echo signal decay of (a) cation and (b) anion species in PVDF membranes with the averaged pore size of 0.1 μm (●) and 5 μm (○) under the pulse sequence for diffusion measurement. Broken lines are fitted results according to eq 2 with two components. Solid lines are fitted results according to eq 5 with a single component for 0.1-μm membrane and with two components for 5-μm membrane.

Results and Discussion

Examination of Possibility of Restricted Diffusion in Observed Echo Attenuation. As we proposed in the previous section of formulation, two possibilities exist to assign diffusive behavior that deviated from a simple random walk feature: a restricted diffusion process and a random walk diffusion composed of multicomponents. Observed echo attenuation represented by the marks in Figures 1 and 2 showed the curved feature different from the monotonic linear change indicating a single component of random walk migration of eq 1. Therefore, we first investigate which model is responsible for the observed feature by the simulation on the restricted diffusion model.

The pore-hopping model, which is an extended geometrical model for restricted diffusion process, is most appropriate to describe the carrier migration situation in the porous structure to confirm the probability of diffusion restriction in PE membranes.[12] We then simulated the echo-changing feature in Figure 3 assuming a pore size of 0.03 μm, 0.1 μm, and 1.0 μm for a and 3×10^{-6} cm^2 s^{-1} for D ($D_{\text{eff}} = 0.23D$: this is a typical assumption in the model). Different pore sizes were selected, on the basis of the order of PE membranes, to see the pore size dependence of echo attenuation for the typical diffusion value of the cation species in a free electrolyte solution. Here, we assumed $b \cong a$ (where b is the mean spacing between pores and a is the mean size of the pores) to describe the porous morphology of the PE membrane, on the basis of the observed SEM photographs. The simulated results demonstrate that,

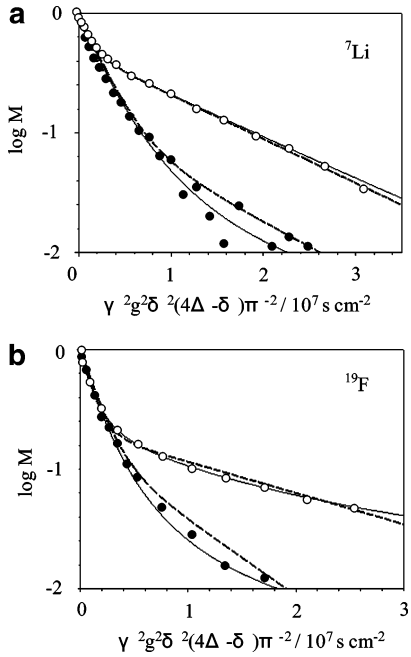

Figure 2. NMR spin−echo signal decay of (a) cation and (b) anion species in PE membranes with the averaged pore size of 0.03 μm (●) and 0.06 μm (○) under the pulse sequence for diffusion measurement. Broken lines are fitted results according to eq 2 with two components. Solid lines are fitted results according to eq 5 with a single component for 0.03-μm membrane and with two components for 0.06-μm membrane.

assuming the practical parameters used in the experiment for these samples, the log-plot of echo intensity changed almost linearly in the detectable attenuation range of observed echo intensity in the experiment (0 to −2 in log-scale). With increasing a value larger than 1.0 μm, the simulation plot became linear approaching to the random walk feature in a pore. With decreasing a value smaller than 0.1 μm, the plot also become linear approaching to the long-range migration randomly with D_{eff}. This reveals that restricted diffusion, even if it exists, cannot be detected as the form of curved feature in echo observation for the PE membranes. That is, the characteristic observed echo decay does not arise from restricted diffusion reflecting the localized geometry of the porous structure. Rather, it is better to infer several diffusive phases or the diffusion distribution attributed to the pore size distribution of the overall membranes.

Diffusion Behavior of Lithium Electrolyte Solution in PVDF Porous Membranes. The marks in Figure 1 represent the spin−echo decays of the cation and anion species of lithium electrolyte in PVDF membranes having the averaged pore size of 0.1 μm and 5.0 μm. The pore size was confirmed from SEM observation. To evaluate the attenuation data, we first assumed a random walk migration having discrete diffusion values represented by eq 2. The broken lines in the figure are the fitted results considering two components ($i = 2$) for eq 2 as a single component fitting did not match to the data. Estimated diffusion values after fitting are listed in Table 1 with their population fraction. The two diffusion components of the small-pore membrane (0.1 μm) were close to each other in contrast to the orderly different values of the large-pore membrane (5 μm). It is presumed that the two diffusion values of large-pore membrane are attributed to two different phases which are independent in carrier migration in the membrane. We next considered the diffusion distribution to reproduce the observed echo attenuation. Fitting with eq 5 for the small-pore membrane

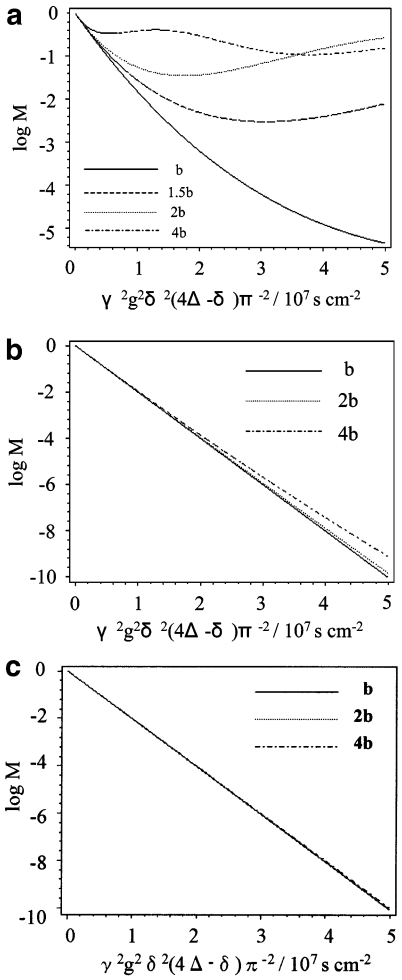

Figure 3. Typical behavior of spin−echo decay of the restricted diffusion process following a pore-hopping model with parameters (a) $a = 1$ μm, $b = 1.1$ μm; (b) $a = 0.1$ μm, $b = 0.11$ μm; and (c) $a = 0.03$ μm, $b = 0.033$ μm, $D_{\text{eff}} = 4.6 \times 10^{-7}$ cm^2 s^{-1}, $\Delta = 80$ ms, $\delta = 0-3$ ms, $g = 1065$ G cm^{-1}.

TABLE 1: Numerical Results of Fitting, Diffusion Coefficient, [Standard Deviation], (Population Fraction in a Sample), for Observed Echo Decay of PVDF and PE Membranes Using the Discrete Exponential Function (Eq 2) and Distribution Function (Eq 5)

	PVDF		PE	
	0.1 μm	5.0 μm	0.03 μm	0.06 μm
discrete diffusion fitting[d]	3.89[a] (54.1%)[c] 1.64 (45.9%)	5.07 (72.5%) 0.90 (27.5%)	4.36 (87.9%) 0.95 (12.1%)	8.47 (51.7%) 0.85 (48.3%)
distribution diffusion fitting[e]	2.69 [0.853][b]	5.08 (72.9%) [0.316] 0.93 (27.1%) [0.190]	4.99 [2.15]	8.62 (52.3%) [1.92] 0.83 (47.7%) [1.24]

[a] The value without any parentheses shows diffusion coefficient, $D/10^{-7}$cm^2 s^{-1}. [b] The value in brackets [] shows standard deviation, $\sigma/10^{-7}$cm^2 s^{-1}. [c] The value in parentheses () shows population fraction of the diffusive component. [d] Fitting using eq 2. [e] Fitting using eq 5. In this fitting, D_0 is listed.

showed a good agreement with the observed decay only with a single component ($i = 1$), which is shown by a solid line in Figure 1. For the large-pore membrane, it was necessary to apply eq 5 with two components ($i = 2$) to reproduce the observed result as in the figure. The averaged diffusion values and theirstandard deviations were summarized in Table 1. The distribution function was plotted in Figure 4 with the discrete

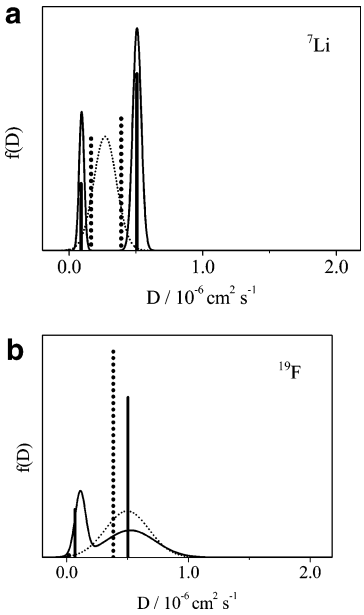

Figure 4. Distribution function of the fitted result according to eq 5 with the vertical lines of the fitted result according to eq 2 of (a) cation and (b) anion species in PVDF membrane. Broken lines are the results for 0.1-μm membrane and solid lines are the results for 5-μm membrane. The area of distribution function of each membrane is normalized to be unity. The length of vertical line of each membrane is normalized to be unity.

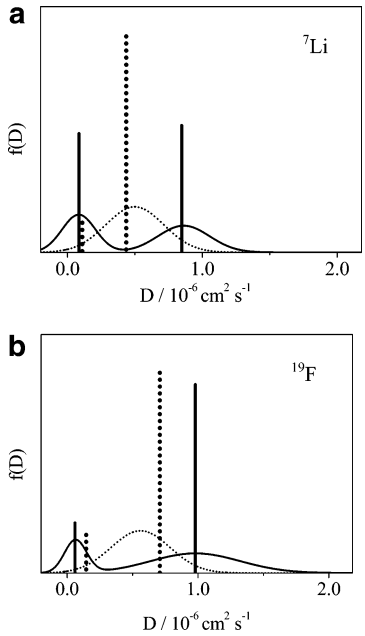

Figure 5. Distribution function of the fitted result according to eq 5 with the vertical lines of the fitted result according to eq 2 of (a) cation and (b) anion species in PE membrane. Broken lines are the results for 0.03-μm membrane and solid lines are the results for 0.06-μm membrane. The area of distribution function of each membrane is normalized to be unity. The length of vertical line of each membrane is normalized to be unity.

values (vertical lines) assuming eq 2. The vertical length or surrounding area of lines for two components corresponds to the population fraction of each diffusion component. It is accepted for the large-pore membrane that the two discrete phases are present. Each phase is characterized by a diffusion value which is distributed in the range of a standard deviation. On the other hand, the fitting with the distribution function for the small-pore membrane showed a high reproducibility with a single component. Considering the close discrete values for the cation and dominant population of high diffusive phase for the anion using eq 2, it is reasonable to assume a single diffusion phase with fairly large distribution for the small-pore membrane.

The phase condition can be supported by the solution insertion process in PVDF membranes. We have already described the two-step progress of gelation process of PVDF porous membranes from observation of echo-changing behavior of diffusion.[15,16] That is, the solution first occupies the pores after the membrane is immersed into the solution. Next, the trapped solution in the pores penetrates into the polymer network through the pore wall to swell the polymer chains. The solution in the pores of a small-pore membrane would disappear at the second step as the swollen polymer walls depress the pores. This results in providing a single diffusive phase of the swollen polymer pathways. On the other hand, two diffusive phases are present in a large-pore membrane: one comes from the residual solution in the interconnected pores which shrank but remained as a result of expansion of the swollen polymer; the other is a result of the swollen polymer network which is similar to that observed in the small-pore membrane. The difference in the absolute diffusion values of the swollen region between the large- and small-pore membranes would be attributed to the difference in polymer network condition. The network of the small-pore membrane is more uniform and expanding in all directions without disturbance of residual pores in the large-pore membrane.

Diffusion Behavior of Lithium Electrolyte Solution in Polyethylene (PE) Porous Membranes. Next, we compare diffusion behaviors of carriers of two PE membranes that had different processing conditions: with and without a plasticizer in stretching to form the porous structure. Average pore sizes of the membranes were roughly estimated to be 0.03 μm and 0.06 μm using the BET adsorption method. Different morphology of membranes was observed by SEM photographs. That is, the small-pore membrane stretched with the presence of a plasticizer was uniform in porous structure; also, the large-pore membrane stretched without a plasticizer looked nonuniform in polymer network density, showing the island structure of submicron to micron size composed of dense (no pore) and thin (porous) phases.

Figure 2 shows spin−echo decay of cation and anion species probed by ^{7}Li and ^{19}F, respectively, in the PE membranes. The decay of the small-pore membrane showed a monotonic curve of downward convex features. When we first tried to fit those results using eq 2 assuming the combination of discrete two diffusion phases as shown by the broken lines in the figure, the fitted results was slightly in disagreement with the experimental data for both membranes. This indicates that we need to improve the fitting function including multicomponents for diffusion. The fitting with the consideration of diffusion distribution using eq 5 showed good agreement with the observed echo change. We assumed a single phase for the small-pore membrane and two phases for the large-pore membrane to obtain the best results. The distribution condition is represented in Figure 5. It appeared that the diffusion distribution is larger in PE membranes for both species compared with the results of PVDF membranes. This suggests that the carrier diffusivity in PVDF membranes is rather uniform. This would be attributable to (1) porous structure determined in the preparation process and (2) the swelling feature of the polymer for the nonaqueous solution. It is accepted that PE polymer does not swell with the solution; it merely retains the inserted solution in the interconnected pores in the membrane. Consequently, the inherent pore size distribution of the membrane is directly reflected in the diffusion values

as diffusion distribution. For PVDF polymer, the solution penetrates partially into the polymer across the wall of the pores to swell the polymer in the vicinity of the walls. This geometrical modification would moderate scatter of the pore size and promote morphological uniformity.

To confirm the two-phase assumption for large-pore membranes, spin−echo observation was performed by changing the diffusion time, Δ from 30 to 160 ms, which is the maximum variable range in this measurement system. The echo-changing behavior was independent of the diffusion time in the range. This indicates that the carrier exchange between the two phases is slow enough to assume them being independent during the measuring time. This result also ruled out the possibility of restricted diffusion manner in which the echo-changing feature apparently depends on Δ.[9]

In conclusion, echo attenuation of carrier diffusion in PE porous separator membranes showed the characteristic feature of a downward convex curve. Using a Gaussian function, NMR echo signal change could be represented as the situation of diffusion distribution. Moreover, the possibility of restricted diffusion process was ruled out by simulating the echo change on the basis of the pore-hopping model and observing the independent echo signal change on Δ. This means that echo-changing behavior does not reflect local space geometry depending on each pore size, but the statistical feature attributed to the pore size distribution. High uniformity of carrier diffusion resulting from geometrical uniformity of host PVDF membranes indicates that polymer swelling would act to average the pore size scattering. Evaluation of diffusion distribution condition by introducing the Gaussian function would be effective for judgment of uniformity of porous structure which determines the fundamental transport performance of membranes.

References and Notes

(1) Venugopal, G.; Moore, J.; Howard, J.; Pendalwar. S. *J. Power Sources* **1999**, *77*, 34.

(2) Abraham, K. M. *Electrochim. Acta* **1993**, *38*, 1233.

(3) Saito, Y.; Kataoka, H.; Capiglia C.; Yamamoto, H. *J. Phys. Chem. B* **2000**, *104*, 2189.

(4) Saito, Y.; Kageyama, H.; Nakamura, O.; Miyoshi, T.; Matsuoka, M. *J. Mater. Sci.* **2000**, *35*, 809.

(5) Saito, Y.; Capiglia, C.; Yamamoto, H.; Mustarelli, P. *J. Electrochem. Soc.* **2000**, *147*, 1645.

(6) Tanner, J. E.; Stejskal, E. O. *J. Chem. Phys.* **1968**, *49*, 1768.

(7) Tanner, J. E. *J. Chem. Phys.* **1978**, *69*, 1748.

(8) Price, W. S. *Annu. Rep. NMR Spectrosc.* **1996**, *32*, 51.

(9) Kataoka, H.; Saito, Y.; Tabuchi, M.; Wada, Y.; Sakai, T. *Macromolecules* **2002**, *35*, 6239.

(10) Watanabe, M.; Sanui, K.; Ogata, N. *Macromolecules* **1986**, *19*, 815.

(11) Ratner, M. A. *Polymer Electrolyte Reviews − 1*; MacCallum, J. R., Vincent, C. A., Eds.; Elsevier Applied Science: London and New York, 1987; p 173.

(12) Callaghan, P. T.; Coy, A.; Halpin, T. P. J.; MacGowan, D.; Packer, K. J.; Zelaya, F. O. *J. Chem. Phys.* **1992**, *97*, 651.

(13) Tanner, J. E. *J. Chem. Phys.* **1970**, *2*, 2523.

(14) Price, W. S.; Kuchel, P. K. *J. Magn. Reson.* **1991**, *94*, 133.

(15) Kataoka, H.; Saito, Y.; Sakai, T.; Quartarone, E.; Mustarelli, P. *J. Phys. Chem. B* **2000**, *104*, 11460.

(16) Saito, Y.; Kataoka, H.; Quartarone, E.; Mustarelli, P. *J. Phys. Chem. B* **2002**, *106*, 7200.